Journal of Engineering Mathematics, Vol. 6, No. 4, October 1972
Wolters-Noordhoff Publishing–Groningen
Printed in the Netherlands

Rayleigh Wave Propagation in a Viscoelastic Half-Space

J. ABOUDI

School of Engineering, Tel-Aviv University, Ramat Aviv, Israel.

(Received November 4, 1971 and in revised form March 6, 1972)

SUMMARY

Rayleigh waves excited by an impulsive force imbedded in a linear viscoelastic half-space are synthesized by applying an approximate inversion of the Fourier transform which yields reliable results. The method is general enough and can be applied to general models of viscoelasticity described by the Boltzmann superposition principle, with a relaxation or creep function given analytically or numerically in the time or frequency domain. Illustrations are given in cases of simple and complicated models of viscoelasticity.

1. Introduction

Only few works appear to deal with three-dimensional dynamic viscoelastic problems (two space variables and time variable) due to mathematical difficulties. See for example a review by Kolsky [1].

The problem of wave propagation in a viscoelastic half-space caused by an impulsive source was treated by Chao and Achenbach [2] for a three-parameter viscoelastic model, under the assumption of a constant Poisson ratio. More recently Tsai and Kolsky [3] studied both theoretically and experimentally the excited surface waves in a viscoelastic half-space caused by the impact of a steel ball. Abubakar [4] obtained expressions for the displacements due to a buried line source, by the application of the multiple saddle point approximation.

In the present work we apply an approximate inversion of the Fourier transform based upon the Cooley and Tukey algorithm [5]. This method has proved to be very efficient and accurate in treating the problem of wave propagation from a spherical cavity in a viscoelastic medium [6]. This is generalized here in order to treat the more difficult case of Rayleigh wave propagation in a viscoelastic half-space due to an impulsive vertical buried force. With this method of inversion we are able to handle any type of linear viscoelastic isotropic half-space having a relaxation or creep function which is given analytically or numerically in the time or frequency domain.

After checking the accuracy of the inversion, the method is illustrated for a viscoelastic half-space of the Maxwell and standard linear solid types, and it is shown that a straightforward generalization can easily be performed for a generalized Maxwell model containing a finite number of elements. This model can also be represented by a stress related to the strain according to linear differential operators with respect to time of finite orders. Next we illustrate it for the more general case of a network containing an infinite number of elements, which corresponds to a stress-strain relation having fractional time derivatives. As a last illustration we present Rayleigh waves in a viscoelastic half-space defined by a logarithmic creep function. This function has the property that it provides a fairly constant loss factor over a large range of frequency, a property which must be imposed according to observational and experimental results. In all these illustrations, the solution is compared with Rayleigh waves in an elastic half-space, and the resulting attenuation and dispersion are shown. The dispersion is also shown in plots of the particle motions (trajectories) resulting in the various models treated.

The present method of solution can easily be applied to other related problems of interest. Thus it was recently shown by Moke [7] that a reinforced material with parallel fibers behaves in certain circumstances as a viscoelastic medium with an effective complex density. Similarly it was shown by Hudson [8] that the scattering of Rayleigh waves by inhomogeneities whose size is small compared with the wavelengths of the incident wave gives rise to an attenuation

caused by a certain viscoelastic law. This law implies that the moduli and density are complex quantities depending on the frequency in a particular manner. Although it is not obvious what is the meaning of complex density, the method presented here can formally handle with ease those viscoelastic laws as well as a density represented by a complex quantity depending on the frequency.

2. Statement and Formal Solution of the Problem

Consider a viscoelastic isotropic half-space containing a buried vertical point force at depth h beneath the surface, see Fig. 1a, whose time dependence is given by $f(t)$, commencing at time

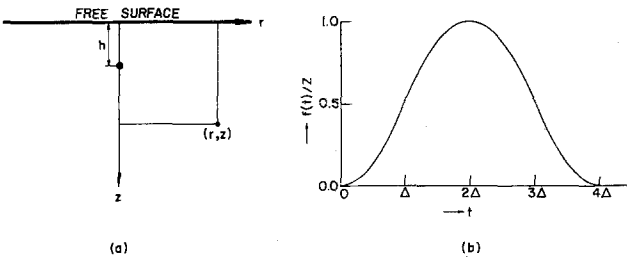

Figure 1 (a). Vertical force imbedded at depth h beneath the surface of a viscoelastic half-space; (b) Time variation of the source function $f(t)$ given by (15).

$t=0$. The viscoelastic half-space is described by the general Boltzmann superposition principle, with the relaxation or creep functions given analytically or numerically in the time or the frequency domain.

The constitutive equations according to this principle are:

$$\sigma_{ij}(t)=\delta_{ij}\int_{-\infty}^{t} G_1(t-\tau)\frac{\partial}{\partial\tau}D(\tau)d\tau+2\int_{-\infty}^{t} G_2(t-\tau)\frac{\partial}{\partial\tau}\varepsilon_{ij}(\tau)d\tau \tag{1}$$

where σ_{ij}, ε_{ij} are the stress and strain tensor components respectively, and $G_1(t)$, $G_2(t)$ are the relaxations function which are zero for $t<0$. δ_{ij} is the Kronecker delta and $D=\operatorname{div}\boldsymbol{u}$ where $\boldsymbol{u}$ is the displacement vector. The initial conditions are: $\boldsymbol{u}=\partial\boldsymbol{u}/\partial t=0$ at $t=0$, representing a quiescent state at $t=0$.

Equation (1) can be rewritten in the following form:

$$\sigma_{ij}(t)=G_1(0)\left\{D(t)-\int_{-\infty}^{t}\dot{\psi}_1(t-\tau)D(\tau)d\tau\right\}\delta_{ij}$$
$$+2G_2(0)\left\{\varepsilon_{ij}(t)-\int_{-\infty}^{t}\dot{\psi}_2(t-\tau)\varepsilon_{ij}(\tau)d\tau\right\} \tag{2}$$

in which the dots represent derivative with respect to argument, and $\psi_1(t)$, $\psi_2(t)$ are defined by:

$$G_i(t)=G_i(0)\{1-\psi_i(t)\}\,,\qquad i=1,2 \tag{3}$$

and therefore $\psi_1(t)=\psi_2(t)=0$ at $t=0$. In the perfectly elastic case G_1, G_2 are time-independent and reduce to the Lamé constants λ, μ respectively. A correspondence principle can be easily obtained from (2) by defining $\xi=t-\tau$ and then extending the lower limit of integration to $-\infty$ obtaining:

$$\sigma_{ij}=G_1(0)D(t)\delta_{ij}+2G_2(0)\varepsilon_{ij}(t)-G_1(0)\delta_{ij}\int_{-\infty}^{\infty}\dot{\psi}_1(\xi)D(\boldsymbol{r},t-\xi)d\xi$$
$$-2G_2(0)\int_{-\infty}^{\infty}\dot{\psi}_2(\xi)\varepsilon_{ij}(\boldsymbol{r},t-\xi)d\xi \tag{4}$$

and $\boldsymbol{r}=(x,y,z)$ is the vector of position.

Applying the Fourier transform with respect to t to (4) and using the convolution theorem we get:

$$F[\sigma_{ij}] = G_1(0)(1-F[\dot{\psi}_1])F[D]\delta_{ij}+2G_2(0)(1-F[\dot{\psi}_2])F(\varepsilon_{ij}] \tag{5}$$

where

$$F[g(t)] \equiv \bar{g}(\omega) = \int_{-\infty}^{\infty} g(t)\,e^{-i\omega t}dt\,. \tag{6}$$

Therefore we obtain in the Fourier transform domain the following correspondence principle between a perfectly elastic problem and the corresponding viscoelastic problem:

$$\left.\begin{aligned}\lambda &\leftrightarrow G_1(0)(1-F[\dot{\psi}_1]) \equiv L(\omega)\\ \mu &\leftrightarrow G_2(0)(1-F[\dot{\psi}_2]) \equiv M(\omega)\,.\end{aligned}\right\} \tag{7}$$

The problem of a vertical force directed along the z-axis and buried within an elastic half-space has a cylindrical symmetry. Therefore all quantities are independent of the azimuthal angle θ of the cylindrical coordinates (r, θ, z) and the displacement vector components at the observation point $(r, z=0)$ are given for the elastic case by, see Pekeris [9] (with different notations)

$$\bar{u}_r(r, 0, \omega) = -\frac{\bar{f}(\omega)}{2\pi\mu}\int_0^{\infty} \frac{2\nu_1\nu_2\,e^{-\nu_1 h}-(2k^2-k_2^2)e^{-\nu_2 h}}{F_0(k)}\,k^2 J_1(kr)dk \tag{8}$$

$$\bar{u}_z(r, 0, \omega) = \frac{\bar{f}(\omega)}{2\pi\mu}\int_0^{\infty} \frac{(2k^2-k_2^2)e^{-\nu_1 h}-2k^2 e^{-\nu_2 h}}{F_0(k)}\,\nu_1 k J_0(kr)dk\,. \tag{9}$$

Here:

$$\nu_i = (k^2-k_i^2)^{\frac{1}{2}} \qquad (i=1,2) \tag{10}$$

$$k_1^2 = \omega^2\rho/(\lambda+2\mu)\,, \quad k_2^2 = \omega^2\rho/\mu \tag{11}$$

$$F_0(k) = (2k^2-k_2^2)^2-4k^2(k^2-k_1^2)^{\frac{1}{2}}(k^2-k_2^2)^{\frac{1}{2}}\,, \tag{12}$$

h is the depth of the source and ρ is the density. It is worthwhile to note that the generalization to vertical forces which are distributed continuously in a circular region is straightforward, see Miller and Pursey [10] for the corresponding expressions to (8) and (9).

By replacing the Bessel function J_n of order n in (8–9) by the Hankel functions of the first and second kind $(H_n^{(1)}+H_n^{(2)})/2$ and transforming the path of integration in the complex k plane [11], then the residue at the Rayleigh pole $k_0=\gamma k_2$ where $F_0(k_0)=0$ yields the Rayleigh wave displacements

$$\bar{u}_r = -\frac{i\bar{f}(\omega)}{2\mu}\left[\frac{2\nu_1\nu_2\,e^{-\nu_1 h}-(2k^2-k_2^2)e^{-\nu_2 h}}{F_0'(k)}\,k^2 H_1^{(2)}(kr)\right]_{k=k_0} \tag{13}$$

$$\bar{u}_z = \frac{i\bar{f}(\omega)}{2\mu}\left[\frac{(2k^2-k_2^2)e^{-\nu_1 h}-2k^2 e^{-\nu_2 h}}{F_0'(k)}\,\nu_1 k H_0^{(2)}(kr)\right]_{k=k_0}\,. \tag{14}$$

According to the correspondence principle (7) we replace the Lamé constants λ, μ in (10–14) in the case of a viscoelastic half-space by $L(\omega)$, $M(\omega)$ respectively. Then (13–14) yield the surface displacements connected with Rayleigh waves caused by a buried vertical force in a viscoelastic half-space, specified by the relaxation functions (3).

Two different cases arise in determining k_0:

(1) Poisson ratio $\sigma=0.5G_1(t)/[G_1(t)+G_2(t)]$ is time-independent, then γ is a constant independent of ω. For example if $G_1(t)=G_2(t)$ then $\sigma=0.25$ and $\gamma=0.5(3+\sqrt{3})^{\frac{1}{2}}$.

(2) Time-indepent Poisson ratio, $\sigma(t)$. In this case γ depends on ω and must be computed for every frequency component by locating the root (generally complex) of $F_0(k)=0$ at that frequency.

In all the illustrations given in the sequel we choose $G_1(t)=G_2(t)\equiv G(t)$ although more general cases can be treated exactly in the same manner.

3. The Temporal Variation of the Source

We consider a vertical point force buried below the free surface of the viscoelastic half-space with a time variation $f(t)$ given by:

$$f(t) = Z\{\Delta_2[p(t)] - \Delta_2[p(t-2\Delta)]\} \tag{15}$$

with

$$p(t) = t^2 H(t)/2 \tag{16}$$

where $H(t)$ is the Heaviside step function, Z is an amplitude factor having the dimension of a force and Δ_2 is a second finite difference operator defined by:

$$\Delta_2[p(t)] = [p(t) - 2p(t-\Delta) + p(t-2\Delta)]/\Delta^2 . \tag{17}$$

The parameter 4Δ is the duration of the pulse, see Fig. 1(b). The Fourier transform of $f(t)$ is given by:

$$\bar{f}(\omega) = 4Z \sin \omega\Delta (1 - \cos \omega\Delta) e^{-2i\omega\Delta}/\omega^3 \Delta^2 \tag{18}$$

and

$$\bar{f}(0) = 2Z\Delta$$

In all the illustrations given in this paper we choose $4\Delta = 30\, h/c_p$, where $c_p^2 = [G_1(0) + 2G_2(0)]/\rho$. Similarly we define: $c_s^2 = G_2(0)/\rho$. All the displacements in these illustrations have the multiplication factor $Z/G_2(0)$.

4. Approximate Method of Inversion

The inversion of the expressions (13–14) for the horizontal and vertical displacements at $z = 0$, back to the time domain is based upon a direct approximation of the inverse transform by a finite sum. For a real causal function, $g(t) = 0$ for $t < 0$, the inverse transform of (6) is given by [12]:

$$g(t) = \frac{2}{\pi} \int_0^\infty \mathrm{Re}[\bar{g}(\omega)] \cos \omega t \, d\omega , \qquad t > 0 , \tag{19}$$

and (19) is approximated by:

$$g(t_k) = \frac{2\Delta\omega}{\pi} \sum_{n=0}^{N-1} \mathrm{Re}[\bar{g}(\omega_n)] \cos \omega_n t_k \tag{20}$$

where $t_k = k\Delta t$, $k = 0, \ldots, K-1$ and $\omega_n = n\Delta\omega$, $n = 0, \ldots, N-1$ with

$$\Delta t = 2\pi/(N-1)\Delta\omega . \tag{21}$$

In (13–14) the angular frequency span ω_N is divided into N equal increments $\Delta\omega$, and the time span t_K in (19) is divided into K equal increments Δt. We set $N = K$ which is a usual case for computing.

We employ the Cooley and Tukey algorithm [5] in evaluating (20). A straightforward numerical evaluation of (20) involves making K multiplications and additions for each of the K values of k, i.e. a total of K^2 operations. Thus the time of calculations is proportional to K^2. The above algorithm reduces considerably the number of operations, allowing the computations to be done in a time proportional to $K \log K$ instead of K^2. This is of course a significant saving for large values of K. Actually the computer program based upon this procedure generates the displacements for all the range $0 \leq t_k \leq t_{K-1}$ in about half a minute on the C.D.C. 6600 computer, for the case $N = K = 2^{13}$.

5. Checking the Accuracy of the Inversion

Let us check the accuracy of the inversion as follows:

(1) The recovery of the function $f(t)$ given by (15) by applying the inversion procedure (20)

to (18). The correspondence between the analytical expression (15) and the numerical values obtained was excellent. The relative errors at the various values of t were less than 1% for $N=2^{13}$.

(2) We examined the displacements obtained with several values of the angular frequency increments and different number of input points N (Fourier components), but such that the frequency span ω_N is kept constant, so that the time increment Δt given by (21) remains constant too. In this way we checked the variations of the numerical values of the two displacement components in the case of a perfectly elastic half-space at the observation point $r/h=10$, $z=0$, in the time interval $20<c_p t/h<40$.

We started with angular frequency increment $h\Delta\omega/c_p=0.0128$, $N=2^8$ and then we refined successively up to $h\Delta\omega/c_p=4\times10^{-4}$, $N=2^{13}$ where the solution showed no appreciable changes. We found that the maximum relative error in the above mentioned time interval was about 4% when refining from 2^8 and 2^9, and it reduced to less than 1% when refining from 2^{12} to 2^{13} Fourier components. Note that these slight changes are indistinguishable up to the scale of the plot.

In the following illustrations we employed $N=2^{13}$ Fourier components in order to synthesize the Rayleigh waves, although one hundred components, starting at a reference frequency ω_0, were used in [3] to compute the stress pulses. The need to such a large number of components is imposed by the requirement to obtain an accurate solution, especially when the relaxation function changes rapidly with time.

Similar error checks were performed in a dissipative case, but these results will be reported in a later section.

6. Maxwell and Generalized Maxwell Models

Let us illustrate first the present method of solution for the simple models of one Maxwell element and a standard linear solid. The relaxation function $G(t)$ for the Maxwell model is given by:

$$G(t)=G(0)\,e^{-t/t_0} \tag{22}$$

where t_0 is a relaxation constant and $G(0)=(c_s/c_p)^2$. In Fig. (2) the vertical and horizontal

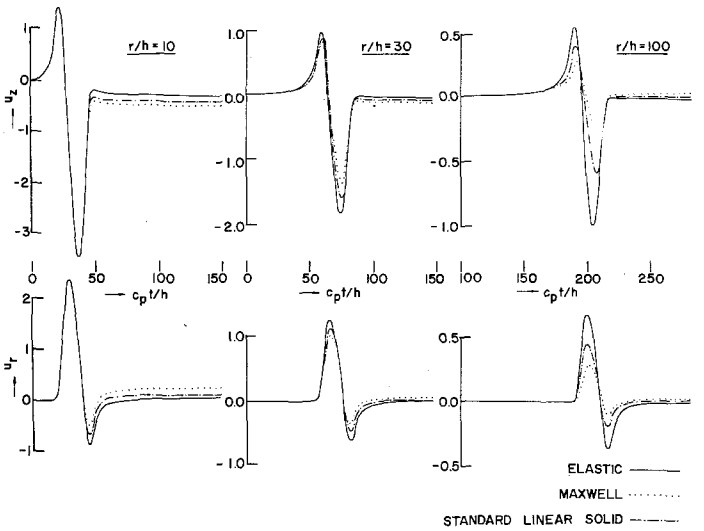

Figure 2. Vertical and horizontal displacements on the surface of a viscoelastic half-space of the Maxwell and standard linear solid type. The elastic case is represented by the solid line.

displacements, connected with Rayleigh waves, on the surface of a viscoelastic half-space characterized by (22) with $c_p t_0/h=100$ containing a vertical point force are shown. The dis-

placements are given at distances $r/h = 10, 30, 100$. The solid curves represent the corresponding displacements in an elastic half-space.

For the standard linear solid we choose the relaxation function:

$$G(t) = G(0)(1 + e^{-t/t_0})/2 . \tag{23}$$

Both (22) and (23) have the same value $G(0)$ at $t=0$, but $G(t)$ in (23) tends to the constant value $G(0)/2$ at $t \to \infty$. The corresponding displacements for the standard linear solid are shown in Fig. (2). These displacements form a partial contribution to the complete solution which contains both body and Rayleigh waves. In the present case of the force of finite duration (15), the complete solution tends to zero for large times. As Rayleigh waves form the dominant contribution to the complete solution for large distances ($r/h \gg 1$), we expect them to produce zero displacements at large times. This is well seen in Fig. (2) and the other Figures of this paper. On the other hand, for small distances Rayleigh waves are not the dominant part of the complete solution. Hence they do not need to tend to zero for large times. This again is clearly seen in the plot of vertical displacements for the small values of r/h.

Whereas these curves show clearly the effect of attenuation, their shape is almost preserved. In order to exhibit the dispersion of Rayleigh waves as a result of the dissipation, the particle motions resulting by combining the vertical and horizontal displacements of Rayleigh waves are given at $r/h = 100$, $z=0$ in Fig. (3a). It is readily seen that the resulting particle motions have quite similar shapes in the both above three cases, and therefore the dispersion is not significant. On the other hand the impulsive excitation of the source yields a non-elliptical path with a cusp, in contradistinction with the case of harmonic Rayleigh waves where the path is retrograde elliptic.

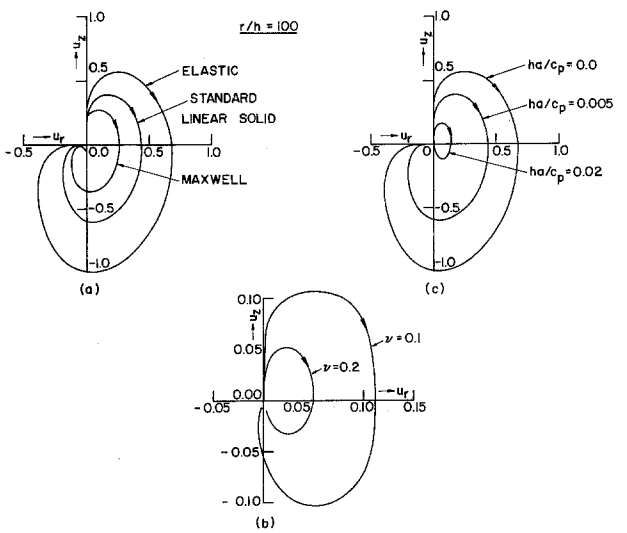

Figure 3. Particle motion on the surface of a half-space of various viscoelastic types.

So far we have illustrated the present technique to simple viscoelastic models, but the generalization to more complicated models which consist of finite number of elements (springs and dashpots) can be easily treated in the same way (the demand to include more elements in the model is needed when dealing with a wider time or frequency range). Such a generalization was shown in [6], in the problem of a cavity imbedded in a viscoelastic medium, for a generalized Maxwell model whose relaxation function is given by:

$$G(t) = G_0 + \sum_{j=1}^{n} G_j e^{-t/t_j} \tag{24}$$

with $n=8$.

In the next section we shall extend the analysis in order to treat a model which contains an infinite number of elements.

7. A Network of Infinite Number Elements

The relaxation function of a generalized Maxwell model is given by (24). As stated before this model can be interpreted in terms of finite number of springs and dashpots. It can equivalently represented by a stress related to the strain by linear differential operators with respect to time of finite orders. Obviously both representations can be treated suitably by the present described method.

Let us apply the present technique to an extended network containing an infinite number of elements. Such a model is given by Bland [13], and consists of a stress-strain relation which contains a fractional time derivative as follows:

$$\sigma = KD^{\nu}\varepsilon\,, \qquad 0 \leqq \nu \leqq 1\,. \tag{25}$$

In this uniaxial relation K is a positive constant, and D^{ν} is a fractional time differentiation of real order ν, defined by:

$$D^{\nu}k(t) = L_p^{-1}[p^{\nu}L_p[k(t)]] \tag{26}$$

where L_p denotes the Laplace transform and p is the transform parameter. The fractional integral according to (26) is given by:

$$D^{-\nu}k(t) = \int_0^t \frac{(t-\tau)^{\nu-1}}{\Gamma(\nu)}\,k(\tau)\,d\tau \tag{27}$$

where Γ is the gamma function.

When $\nu = 0$ we obtain back the perfectly elastic case, and when $\nu = 1$ we get the perfectly viscous case. The complex modulus appropriate to (25) is given by:

$$Y(i\omega) = K(i\omega)^{\nu} = K\omega^{\nu}\left(\cos\frac{\nu\pi}{2} + i\sin\frac{\nu\pi}{2}\right). \tag{28}$$

Let us compute the Rayleigh waves response to a buried force in a viscoelastic half-space described by the present model, such that

$$L(\omega) = M(\omega) = G(0)(i\omega)^{\nu}\,, \quad G(0) = (c_s/c_p)^2 \tag{29}$$

with $L(\omega)$, $M(\omega)$ defined by (7).

In Fig. (4) the vertical and horizontal displacements are given for the two values $\nu = 0.1, 0.2$. The corresponding displacements for an elastic half-space are also shown for comparison ($\nu = 0$). As can be expected the attenuation is more pronounced for the larger value of ν, the

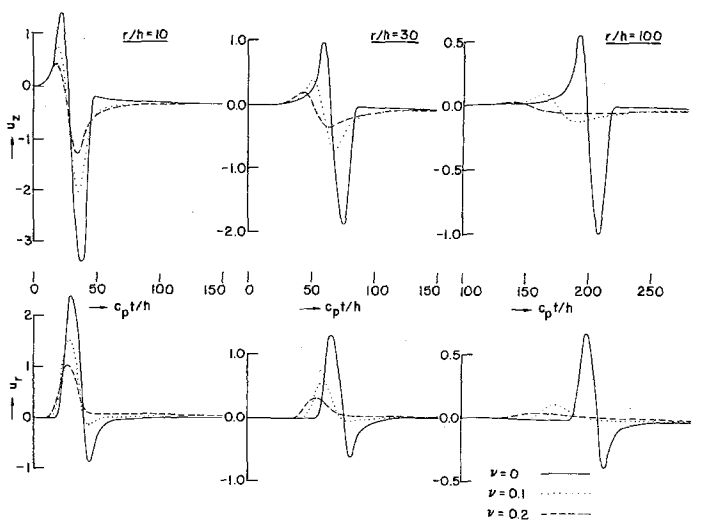

Figure 4. Same as Fig. (2) for a model containing an infinite number of elements.

pulses are extremely broadened as a result of the dissipation. This broadening effect is more significant at the larger distances from the source.

The particle motions of Rayleigh waves corresponding to these two values of v are shown in Fig. (3b). They show clearly the dispersion effect, since the trajectories are completely distorted as compared with the corresponding elastic case.

8. Logarithmic Creep Function

Let us consider a viscoelastic half-space whose dissipation is described by a logarithmic creep function $J(t)$ given by:

$$J(t) = J(0)\{1+\phi(t)\} \tag{30}$$

with

$$\phi(t) = q \log(1+at) \tag{31}$$

where q is a non-dimensional constant and a is a parameter which has the dimension of a frequency.

Observational and experimental results showed that real solids have a loss factor Q^{-1} (or the internal friction) which is quite constant over a wide range of frequencies, see Kolsky [14] and Knopoff and MacDonald [15]. It was shown by Lomnitz [16] that $1/Q$ connected with the creep function given by (30–31) remains relatively constant over a wide range of ω. For the explicit dependence of Q on ω see Lomnitz [17].

In order to obtain the Rayleigh waves displacement in a viscoelastic half-space characterized by (30–31), the corresponding relaxation function $G(t)$ must be constructed. This is easily accomplished according to the following relation between the creep and relaxation function:

$$F[\dot{\psi}(t)] = F[\dot{\phi}(t)]/(1+F[\dot{\psi}(t)]) \tag{32}$$

and

$$G(0) = 1/J(0)\,.$$

The Fourier transform of $\dot{\phi}(t)$ is given by:

$$F[\dot{\phi}(t)] = q\,e^{i\omega/a}\{i\,s_i(\omega/a) - C_i(\omega/a)\} \tag{33}$$

where s_i, C_i are the sine and cosine integral functions as defined by Abramovitz and Stegun [18]. Having $F[\dot{\psi}(t)]$, $L(\omega)$ and $M(\omega)$ in (7) are accordingly determined, then the formal expressions for the displacements can easily inverted.

The present case includes the transition from the creep function to the relaxation function,

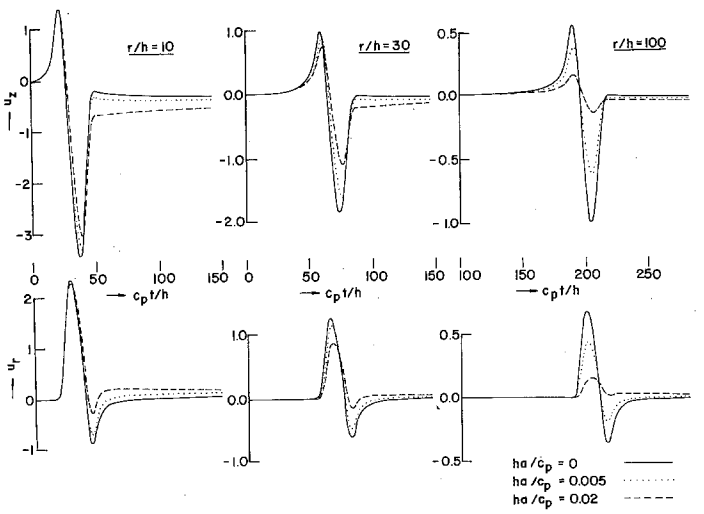

Figure 5. Same as Fig. (2) for the logarithmic creep model.

see eq. (32). Accordingly we compared the resulting displacements by applying the previously described successive refinements number of Fourier components, while keeping ω_N constant. This comparison was performed at $r/h=10$ with $q=1$ and $ha/c_p=0.02$, in the time interval $20<c_p t/h<40$. We found that the maximum relative error between the two cases $N=2^{12}$ and $N=2^{13}$ over all the mentioned time interval is less than 4%, which is larger than the resulting relative error (1%) in the corresponding elastic case reported before. But as in the previous case it is still up to the scale of the plot impossible to distinguish between the two compared curves. We can conclude therefore that the inversion procedure, when it also includes the transition (in the frequency domain) from the creep to the relaxation function, still yields reliable results.

In Fig. (5) the displacements associated with Rayleigh waves are given for $q=1$ and two values of the parameter a: $ha/c_p=0.005$, 0.02, together with the perfectly elastic case ($a=0$) shown for comparison. It is seen that the dissipative effect increases with a, as can be expected. The particle motion for these values of a are displayed in Fig. (3c) at the observation point $r/h=100$, showing clearly the effect of dispersion. The broadening effect can easily be seen in Fig. (5), but it is less pronounced as in the previous model shown in Fig. (4).

Acknowledgment

The computations connected with this paper were performed at the Computations Center of Tel-Aviv University.

REFERENCES

[1] H. Kolsky, The Propagation of Stress Waves in Viscoelastic Solids, *Applied Mechanics Surveys* (1966) 841–846.
[2] C. C. Chao and J. D. Achenbach, A Simple Viscoelastic Analogy for Stress Waves, *Stress Waves in Anelastic Solids*, H. Kolsky and W. Prager (Eds.), Springer, Berlin (1964) 222–238.
[3] Y. M. Tsai and H. Kolsky, Surface Wave Propagation for Linear Viscoelastic Solids, *J. Mech. Phys. Solids*, 16 (1968) 99–109.
[4] I. Abubakar, On the Buried Source in a Viscoelastic Half-Space, *Pure Appl. Geophys.*, 72 (1969) 51–60.
[5] J. W. Cooley and J. W. Tukey, An Algorithm for the Machine Calculation of Complex Fourier Series, *Math. Comp.*, 19 (1965) 297–301.
[6] J. Aboudi, Propagation of Transient Pulses from a Spherical Cavity in a Viscoelastic Medium, *Int. J. for Num. Meth. in Eng.* 4 (1972) 289–299.
[7] C. H. Moke, Effective Dynamic Properties of a Fiber-reinforced Material and the Propagation of Sinusoidal Waves, *J. Acoust. Soc. Am.*, 46 (1969) 631–638.
[8] J. A. Hudson, The Attenuation of Surface Waves by Scattering, *Proc. Camb. Phil. Soc.*, 67 (1970) 215–223.
[9] C. L. Pekeris, The Seismic Surface Pulse, *Proc. Nat. Acad. Sci.*, 41 (1955) 469–480.
[10] G. F. Miller and H. Pursey, The Field and Radiation Impedance of Mechanical Radiators on the Free Surface of a Semi-Infinite Isotropic Solid, *Proc. Roy. Soc. A*, 223 (1954) 521–541.
[11] M. Ewing, W. Jardetzky and F. Press, *Elastic Waves in Layered Media*, McGraw-Hill Book Company, New York (1957) 132–135.
[12] A. Papoulis, *The Fourier Integral and its Applications*, McGraw-Hill Book Company, New York (1962).
[13] D. R. Bland, *The Theory of Linear Viscoelasticity*, Pergamon Press, Inc., New York (1960).
[14] H. Kolsky, *Stress Waves in Solids*, Dover Pub., New York (1952).
[15] L. Knopoff and G. J. F. MacDonald, Attenuation of Small Amplitude Stress Waves in Solids, *Rev. Mod. Phys.*, 30 (1958) 1178–1192.
[16] C. Lomnitz, Linear Dissipation in Solids, *J. Appl. Phys.*, 28 (1957) 201–205.
[17] C. Lomnitz, Application of the Logarithmic Creep Law to Stress Wave Attenuation in the Solid Earth, *J. Geophys. Res.*, 67 (1962) 365–368.
[18] M. Abramovitz and I. A. Stegun, *Handbook of Mathematical Functions*, Dover Pub., Inc., New York (1965).